NONLINEAR FINITE ELEMENT ANALYSIS OF FLUTTERING PLATE IN TRANSONIC UNSTEADY POTENTIAL FLOWS

I Wayan Tjatra , Rendy Kurniawan

Aerodynamics Laboratory , Inter University Center for Engineering Sciences
Institut Teknologi Bandung
Jl. Ganesha 10 , Bandung 40132 , Indonesia

Abstract

An efficient finite element formulation and solution procedure are developed to analyze a nonlinear fluttering isotropic homogeneous plate in unsteady transonic potential flows. The nonlinear governing equation of plate motion are derived from the Lagrange's energy equations in which all forces are presented in term of the plate transverse displacements. Plate stiffeness , stability stiffness , geometrical stiffness and mass matrices are formulated using rectangular elements. The unsteady aerodynamic pressure at each of the elements nodal point are computed based upon the velocity potential obtained from the solution of the unsteady three-dimensional transonic small disturbance flow equations. An iterative linearized approach is employed for the solution of the nonlinear flutter equation. The plate stability behavior are analyzed from the response parameter of the complex eigensolutions. Effects of aerodynamic damping , plate mass distribution , boundary support conditions and initial in-plane forces are investigated.

Introduction

Phenomenon of a fluttering plate is a self-excited oscillation of an external relatively thin skin exposed to an airflow along its surface. Linear plate flutter analysis indicate that there is a critical value of the airflow dynamic pressure above which the plate become unsteable, with motion amplitude grows exponnetially with time. An extensive review of works done on linear plate flutter by Dowell is given in ref. 1 , meanwhile Dugundji[2] presented the theoretical considerations of (linear) plate flutter at high supersonic flows. At present , a great quantity of literature on linear plate flutter are available.

In reality, it is possible that the flutter oscillations will have a large amplitude in which the geometrical nonlinearity effects , mainly due to midplane stretching forces , could restrain the motion of the plate and bound it into a limit cycle oscillation. For accurate assessments and investigation of plate under undergo this kind of motion , the analysis based on nonlinear structural theory with appropriate aerodynamics model must be used.

Several analytical techniques have been developed to investigate nonlinear fluttering plate. Most of them usually use the Galerkin's method in the spatial domain , the modal approach with direct numerical integration , the perturbation method and the theory of harmonic balance commonly use in nolinear dynamics analysis. Each of these methods has their limitations , such as the complexity of mathematical manipulation required , isotropicality and edge boundary conditions of the plate. Lately, finite element method gaining widespread acceptance because of its flexibility in handling geometry , boundary conditions , elastic properties of the plate and flow angularity and the increasing capability of computers hardware. Olson[3] and Sanders[4] , are among the first who developed finite element methods for two and three-dimensional linear plate flutter analysis. An extension of this method into nonlinear oscillation of two and three-dimensional isotropic plate is given by , among others , Mei[5] , and Sarma[6] , for isotropic plate and by Dixon[7] , for laminated composite plate. Temperature effects has also been considered by Xue and Mei as reported in ref. 8. Rectangular or triangular elements are commonly used for simplicity of the finite element formulation.

At present, all of the plate flutter analysis , linear and nonlinear , employed a linearized quasi-steady aerodynamics theory in which the aerodynamics pressure on the surface of the plate are calculated based upon the inviscid potential flow equations. Olson use **Lighthill linearized piston theory** with flow Mach number considered are approximately above 1.6 . Yang[9] developed a finite element procedure using the exact two-dimensional linearized theory (strip theory) for plate flutter analysis in supersonic flows. The use of linearized quasi-steady theory limits the analysis to high supersonic or low subsonic speeds with small oscillation

amplitude. On the otherhand , the most critical speed in plate flutter is the transonic - low supersonic regime[10] . In this speed regime, flow unsteadiness and phase lag between structural motion and aerodynamic response (due to the presence of shock-waves) have a stong influence in the aerodynamic force characteristics. A nonlinear aerodynamics theory is required to take into account these two flow parameters which could not represented completely in the linearized potential flow equations.

A finite element analysis of large amplitude fluttering plate in transonic potential flow is presented here. The governing nonlinear equations of motion are derived from Lagrange potential energy equation in which all forces are formulated in term of transverse displacements of the rectangular plate elements. The plate is conditived to be isotropic, homosoneuos the aerodynamics pressure on each of these elements are computed based upon the velocity potential obtained from the solution of the unsteady three-dimensional transonic small disturbance flow equation. A linearized iterative approach is employed for the solution of the nonlinear flutter equations. The plate stability behavior are analyzed based on the response parameters of the complex eigensolutions. Effects of aerodynamic damping, mass distribution , boundary support conditions and initial in-plane forces are investigated. Comparison are made to the available results wherever possible.

Governing Equations

Plate structure of length a, width b, thickness h, and mass per unit volume m , is represented by a flat panel with airstream flowing over the upper surface in the positive direction of x . at free stream Mach number M , as shown in figure 1. Air flow effects in the lower surfaces is neglected. Plate edges are either simply supported or clamped. Using rectangular elements with six degree-of-freedom per node , the plate is discretized into a certain number of elements. The element nodal displacements vector consists of two components , which are the bending (out of plane , w_b) and membrane (in plane , w_m) displacement components . Bending displacement is comprised of w , w_x , w_y , w_{xy} and the membrane component is comprised of u and v . Strain energy U of the isotropic homogenous plate is written as

$$U = \frac{D}{2}\iint_A \{\Delta^2 w\}dA + \frac{3D}{h^2}\iint_A \left\{\left(u_x + \frac{1}{2}w_x^2\right) + \left(v_y + \frac{1}{2}w_y^2\right)\right\}^2 dA - \frac{3D}{h}\iint_A \left\{\left(u_x + \frac{1}{2}w_x^2\right) + \left(v_y + \frac{1}{2}w_y^2\right)\right\}\left(w_{xx} + w_{yy}\right) dA \qquad [1]$$

in which the nonlinear strain components are formulated using the nonlinear relations as

$$\varepsilon_x = u_x + \frac{1}{2}w_x^2 - z\,w_{xx} \qquad [2.a]$$

$$\varepsilon_x = u_y + \frac{1}{2}w_y^2 - z\,w_{yy} \qquad [2.b]$$

The kinetic energy T is given as function of the plate motion velocity as

$$T = \frac{1}{2}m\iiint_V \left(\dot{u}^2 + \dot{v}^2 + \dot{w}^2\right) dv \qquad [3]$$

where symbol ($\dot{}$) denotes derivation with respect to time. Virtual work ΔW of the aerodynamic pressure due to virtual displacement δw is given by expression

$$\delta W = \iint_A \Delta p(x,y,t)\,\delta w(x,y,t)\,dA \qquad [4]$$

The total aerodynamic pressure on the surface of the plate $\Delta p\ (x,y,t)$ at transonic free-stream Mach number are obtained from the solution of transonic small disturbance (TSD) equation. The plate equations of motion are obtained from Lagrange's energy equation which is

$$\frac{d}{dt}\left(\frac{\partial T}{\partial \dot{q}_j}\right) - \frac{\partial T}{\partial q_j} + \frac{\partial v}{\partial q_j} = Q_j, \quad j = 1,2,\ldots\ldots,n \qquad [5]$$

In this equation Q_j represent the plate generalized forces derived from the virtual work done by the aerodynamic surface pressure. The governing equations are formulated following the simplification procedure adopted by Sarma , as explained in ref. 5 , which can be written in matrix form as

$$[M]\{\ddot{w}\} + \{[K_L] + N_x[K_{NL}]\}\{w\} + \beta[\bar{A}] = 0 \qquad [6]$$

where $[M]$ is the mass matrix , $[K_L]$ is the linear stiffness matrix , $[K_{NL}]$ is the nonlinear stiffness matrix , $[\bar{A}]$ is the aerodynamic force matrix , β is the dynamic pressure parameter , $\beta = q/D$, and D is the bending stiffness coefficient of the plate. Displacement vector $\{w\}$ contains all nodal degree of freedom in the plate. The in-plane (membrane) force , N_x , is defined as

$$N_x = \frac{3D}{h^2}\iint_A \left(w_x^2 + w_y^2\right)dA \qquad [7]$$

Elements of the aerodynamic force matrix, $[\bar{A}]$ will be derived later in the following chapter.

The solution of equation [6] is determined by assuming that the plate motion at the stability boundary is harmonic and can be written as

$$\{w\} = \{w_o\}e^{\Omega t} \qquad [8]$$

The vector $\{w_0\}$ is in general complex, vector so does the plate motion frequency parameter, $\Omega = \alpha + i\omega$. The α variable represent the damping coefficients and ω represent the motion frequency. These two coefficients, α and ω , will determine the characteristics of the plate stability. Substituting the assumed response into eq. [6] results in the governing nonlinear eigen value equation which then be written as

$$\{\kappa [M]+[K_L]+N_x[K_{NL}]+\beta[A]\}\{w_o\}= 0 \qquad [9]$$

in which k is the motion reduce frequency .

Generalized Aerodynamic Forces

The total aerodynamic pressure, Δp (x,y,t), can be expressed, assuming that the load superposition principle is valid, as the sum of the contribution due to each mode shapes, h_j (t). Therefore, the finite state representation of the pressure is written as

$$\Delta p(x,y,t)= \sum_{j=1}^{n} \Delta p_j(x,y,t).h_j(t) \qquad [10]$$

where Δp_j (x,y) represents the total pressure at discrete point (x,y) due to the wing displacement in the j-th mode. Using this relation, the generalized aerodynamic forces for mode -j can be formulated as.

$$Qj = - q \sum_{j=1}^{n} h_j(t) \left[\iint_A \frac{\Delta p_j(x,y)}{q} h_i(x,y)\, dA \right] \qquad [11]$$

in which q is the flow dynamic pressure
The motion generalized forces are then, deduce from equation (11) as

$$\{Q\} = [A]\{w_o\} \qquad [12]$$

$$A_{i_j} = - q \iint_A \frac{\Delta p_j(x,y)}{q}. h_i(x,y)\, dA \qquad [13]$$

where A_{ij} may be considered as the generalized force coefficients from the pressure induced by mode-j acting through the displacement of mode-i. This aerodynamic force coefficient is a function of reduced frequency, k , and usually has complex values. The total aerodynamic pressure for the-j-th mode, Δp_j (x,y,t), it selft is evaluated based on the velocity potential at each rectangular element from the solution of the TSD flow equations,

$$\Delta p_j(x,y,t) = q\left[C_{p_u}(x,y,t) - C_{p_l}(x,y,t)\right] \delta A$$

Where C_{p_u} and C_{p_l} represents the upper and lower surface pressure coefficient, respectively. The coefficient is defined as

$$C_{p_u}(x,y,t) = -2\phi_x - 2\phi_t - \left(1-M^2\right)\phi_x^2 - \phi_y^2 \qquad [14]$$

where ϕ (x,y,t) is the velocity potential. For the plate flutter problem, the aerodynamic flow at the lower surface are neglected that C_{p_l} is equal to zero .

Numerical evaluation of the velocity potential, ϕ , from the TSD solutions employs an approximate factorization (AF) implicit finite difference algorithm developed by Batina[11] , which is proven to be more efficient, accurate and stable compare to other methods. This algorithm consists of a time linearization step to determine an estimate values of the perturbation potential coupled with Newton iteration to provide time accuracy of the solution. Detail about this method is given in ref. 12 . Once the velocity potential are obtained for each element for each mode the aerodynamic force matrix for the whole plate can be formulated.

Solution Procedure

The governing equation of motion , equation [9] , degenerates to the equation of nonlinear vibration problem when $\beta = 0$, and to that of a linear plate flutter problem when the membrane force $N_X = 0$. This equation [9] is a complex eigenvalues problem in which the eigenvalues , k , are obtained for a given value of aerodynamic pressure coefficients. With the increase in the β values , the two eigenvalues coalesce to the critical value, κ_{cr} . The critical dynamic pressure , β_{cr} , at the stability boundary is considered to be the lowest value of β at which coalescence occurs among all values of the eigen-frequencies of the motion.

An iterative procedure and equivalent linearization technique is employed in determining the eigenvalues , κ , which is can be described briefly as follows. The linear flutter equation (with $N_X = K_{NL} = 0$) is first solved ,

$$\left\{\kappa[M]+\left[K_L\right]+\beta[A]\right\}\left\{w_o\right\} = 0 \qquad [15]$$

where $\{w_o\}$ represents the linear mode shape normalized by its maximum components. The iteration process is started by approximating the first displacement vector as

$$\{w_o\} = a\{\bar{w}_o\}e^{\Omega t}$$

where a is the normalized oscillation amplitude of the plate. An equivalent nonlineear stiffness matrix , $[K_{NL}]$, and the nonlinear stretching force , N_X , are then calculated from eq. [7] . The nonlinear flutter solutions are obtained from the linearized eigenvalue equation of the form

$$\{\kappa_i[M] + [K_L] + N_x[K_{NL}] + \beta[A]\}\{w_o\}_i = 0 \qquad [16]$$

where κ_i and $\{w_o\}_i$ are the eigenvalue and eigenvector at the i-th iteration. This iterative process can be repeated until a convergence criterion is satisfied , which are the maximum value and frequency norms of the response. Convergence of the solution is considered achieved whenever any one of these norms reaches a value of 10^{-3} The whole procedure is repeated for several values of dynamic pressure parameter. The critical value of κ is determined from the coalescence point in the β versus κ plots.

Calculation Results

Various numerical examples of plates with hinged-hinged, clamped-clamped, clamped-hinged, and hinged-clamped side conditions have been worked out using the linearized approach proposed. Plate structure with two sides free and the other two hinged and/or clamped (Case A) are modeled as a 9-elements plates , meanwhile plate with all of its sides hinged and/or clamped (Case B) are modeled as a 12-elements plate. To study the accuracy of the elements modeling for plate in Case A , calculation is also carried out using beam elements modeling. Plate elements are assumed as beams which are wide enough that the elastic stiffness of the beam could be replaced by the elastic stiffness of the plate elements, which is

$$k \approx EI \rightarrow D = Eh^3 / 12(1-\nu^2)$$

This beam model was proposed by Olson[3] and Sarma[6] and used for flutter analysis of plates with hinged-free and clamped-free side conditions (cylindrical deformations) which was shown to be accurate. Numerical results for the first two eigenvalues at $\beta = 0$, and for the coalesence (critical values) for the four types of the plate boundary conditions of Case A are shown in Table 1. The four-elements beam model give , in general , a closer natural frequency values to the exact values compared to the plate-element model. This should be the case since the exact values are calculated based on beam model . Comparison of results for the four different side conditions with their exact values shows a larger differences are obtained for plate with stronger side conditions (clamped - clamped). It is seen that the approximate results using the nine-elements plate model and four-elements beam model are in very good agreement with the exact results given in ref. 3. Therefore, nine element plate model was used in all flutter analysis of case A plate presented.

For plate in case B (plate with four side conditions) , good accuracy results of the plate natural frequencies are obtained for model using at least 16 plate-elements, as shown in Table 3. Therefore , for the plate in case B , a 16 elements plate modeling was used for further flutter analysis.

A. Plate with two side - conditions

Plots of the non-dimensional eigenvalues versus dynamic pressure for a clamped-clamped and hinged-hinged plates are given in Figure 1. This plot is typical for any other side conditions. Complete aeroelastic behavior of the plate is characterized by plotting the (complex) eigenvalues variation with increasing (nondimentional) dynamic pressure , from which the motion frequency and damping factor are obtained as,

$$\frac{\Omega}{\omega_0} = (\alpha + i\omega)/\omega_0 = \left(-\frac{1}{2}g_A + \kappa_r\right) + i\left(\kappa_I/2\kappa_r\right)$$

A typical plot is shown in Figure 2. Flutter instability , for the case of negligible aerodynamic damping , g_A equal to zero , is defined to set in when the two undamped natural frequencies merged. For cases where some damping is present, instability set in at a somewhat higher value , as indicated in Figure 3 , which is when the real part of the complex eigenvalue is equal to zero , $\alpha = 0$. As discussed earlier, due to the nonlinear behavior of the plate, this flutter instability is not catashtropic. Response behavior of the plate characterized by a limit cycle oscillation with corresponding frequency $\omega = (\kappa_{real})^{1/2}$. The critical eigenvalues and non-dimensional dynamic pressure of the plate at point of instability for the four types of side condition is summerized in Table 2. Plate with clamped condition of both side has the highest values of critical frequency and dynamic pressure , with the clamped-free plate has the lowest of the two. The clamped-hinged and hinged-hinged plate stand in between. Comparing with the exact solutions, the 16-elements plate model analysis gives a lower of both values values., but the difference is not more than 4% in dynamic pressure and 5.5% in eigen-frequency. Both results shows good agreement with numerical results given by Sarma[6] and Mei[5]. Typical plate deformation mode at the instability boundary is shown in Figure 4 for both clamped-clamped and hinged-hinged plate. The flutter speed of the plate increase almost exponentially as its thickness increased, as shown in Figure 5.

B. Plate with four side - conditions

For plate in case B , four type of side-conditions are considered, which are : all side are hinged or clamped (SSSS or CCCC) , one side is clamped and the rest are hinged (CSSS), and two opposite side are hinged with the other two are clamped (CSSC). The first two natural frequency and the critical response frequency and dynamic pressure at the instability point for zero aerodynamic damping are given in Table 3. In general, the numerical results of this analysis are in good agreement with the results given by Sarma[6] . It is seen that the change in end-condition from hinge to clamp cause an increase in both critical dynamic pressure and eigen-frequency. This increase is more significant for the case in which the clamped side-conditions is perpendicular to the flow direction (CSSS). Shape of the plate deflection when the instability set in are shown in Figure 6 , for SSSS and CSSC side-conditions. Variation of the response frequencies and damping factor are shown in Figure 7 for zero aerodynamic damping conditions. Typical plots are observed for different side-conditions. It can be seen that instability (zero damping condition) of plate with stronger side-conditions occur at higher dynamic pressure and eigen-frequency. Effects of aerodynamic damping (g_A) on critical dynamic pressure of a plate is also studied. It was observed that an increase in g_A value will increase the critical dynamic pressure significantly but almost has no effect on the critical eigen-frequency of the plate.
Figure 8 shows a typical time response of the plate. At point slightly below instability , response tend to converge and as it is approacing the instability point, amplitude of the response increases (slowly) and built a limit cycle type of oscillation. This process continue until a critical dynamic pressure is reached which corresponds to a given limit cycle amplitude. Variation of the critical flutter speed with plate thickness is shown in Figure 9. This results suggest that the plate flutter speeds increase exponentially with its thickness.

Conclusions

A nonlinear finite element procedure for panel flutter analysis in transonic flows has been developed. Several numerical calculation has been performed which shows the effectiveness of the formulation. Based on the preliminary result obtained , the following conclusions may be made.

a. The generalized aerodynamic forces based on the three-dimensional transonic small disturbance solution can be used in the flutter analysis of plate in transonic flow regime. It gives an accurate prediction of the air-load forces on the top surface of the plate. The finite state formulation of the aerodynamic forces employed in this analysis is simple and straightforward. this can be considered to be an improvement over the large number procedure available that use simple aerodynamic theory with restricted range of applicability.

b. The finite element procedure used in this study directly solve for the flutter frequencies. and response mode shapes. No natural frequencies and mode shapes calculation needed, such as in the method of modal analysis.

c. Present results shows that flutter characteristics of nonlinear plate in nonlinear transonic flows are similar to that of nonlinear lifting surface . Flutter of nonlinear plate is not catastrophic which is characterized by a limit cycle type of oscillation.

Acknowledgment

This work is partially supported by the National Research Council (DRN) of Indonesia through the RUT II projects.

References

1. Dowell , E.H. , "Panel flutter : a review of aeroelastic stability of plates and shells" , AIAA Journal , vol. 8 , no. 3 , March 1970.
2. Dugundji , J. , "Theoretical consideration of panel flutter at high supersonic Mach number" , AIAA Journal , vol. 24 , no 7 , July 1977.
3. Olson , M.D. , "Finite elements applied to panel flutter" , AIAA Journal , vol. 5 , no. 12 , Dec. 1967.
4. Sander , G , et.al. , "Finite element analysis of supersonic panel flutter" , *International Journal for Numerical Methods in Engineering* , vol. 7 , Nov. 1973.
5. Mei , C. , "A finite element approach for nonlinear panel flutter" , AIAA Journal , vol. 15 , no. 8 , Aug. 1977.
6. Sarma , B.S. , and T.K. Varadan , "Nonlinear panel flutter by finite element method" , AIAA Journal , vol. 26 , no. 5 , May 1988.
7. Dixon , I.R. , and C. Mei , "Finite element analysis of large-amlitude panel flutter of thin laminates" , AIAA Journal , vol. 31 , no. 4 , Apr. 1993.
8. Xue , D. , and C. Mei , "Finite element nonlinear flutter and fatigue life of 2-D panels with temperature effects" , *Proceedings of the 32nd Structures, Structural Dynamics , and Materials Conference* , Washington DC , Apr. 1991.
9. Yang , T.Y. , and S.H. Sung , "Finite element panel flutter in three-dimensional supersonic unsteady potential flow" , AIAA Journal , vol. 15 , no. 12 , Dec. 1977.
10. Yang , T.Y. , "Flutter of flat finite element panels in a supersonic potential flow" , AIAA Journal , vol. 13 , no. 11 , Nov. 1975.

11. Batina, J.T. , "An efficient algorithm for solution of the unsteady transonic small disturbance equation" , NASA TM 89014 , Dec. 1986.
12. Tjatra , I.W. , "Transonic aeroelastic analysis of system with structural nonlinearities" , Ph. D. Thesis Dept. of Aerospace and Ocean Engineering , Virginia Polytechnic Institute and State University, Blacksburg , Virginia , Apr. 1991.

Boundary	3 x 3 Plate model		Beam model		Exact	
	ω_1	ω_2	ω_1	ω_2	ω_1	ω_2
SFFS	96,030	1582.34	97,460	1570,87	97,4091	1558,55
CFFC	502,985	3932.39	501,893	3874,23	500,564	3803,54
CFFS	236,730	2568.99	238,021	2527,73	237,72	2496,50
CFFF	12,2864	476,309	12,3619	486,65	-	-

Table 1 . The first two eigenvalue of plate and beam model at $\beta = 0$.

Boundary	β critical			K critical		
	Present	Mei	Sarma	Present	Mei	Sarma
CFFC	636.436	636.437	636.570	2721.37	2721.38	2741.40
SFFS	342.346	342.347	343.36	1043.47	1043.47	1051.80
SFFC	478.726	-	479.56	1732.63	-	1746.80
CFFS	478.726	-	-	1732.63	-	--

Table 2 . Critical dynamic pressure and frequency of the plate with various end-conditions.

Boundary	β = 0		Instability	
	ω_1	ω_2	β_{cr}	Ω_{cr}
SSSS	2128.72	3975.9	480.37	3422.75
CSSS	2279.13	4875.6	604.36	4086.45
CCCC	1879.59	6160.3	952.05	5099.07

Table 3. Critical values of dynamic pressure and eigen-frequency for plate with four side-conditions.

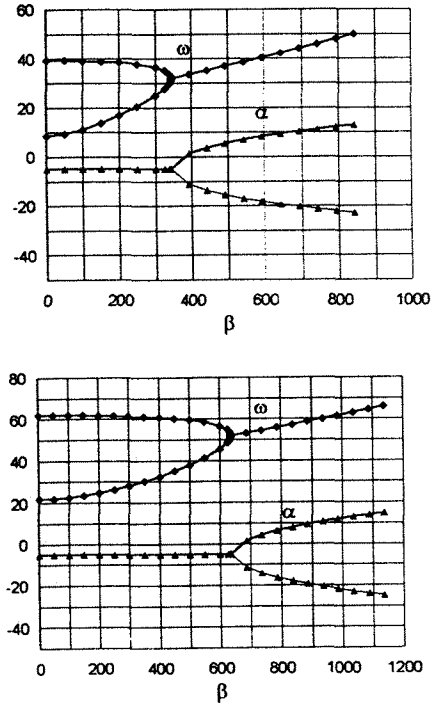

Figure 2. Variation of motion frequency and damping factor with dynamic pressure : a). Hinged-hinged plate, b). clamped-clamped plate.

(hinged-hinged)

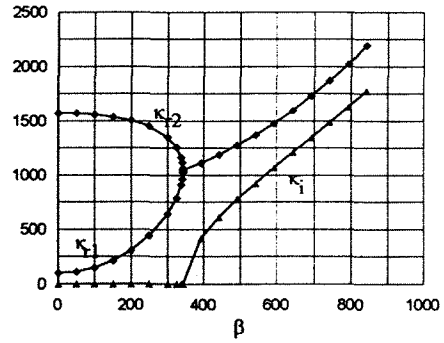

(clamped-clamped)

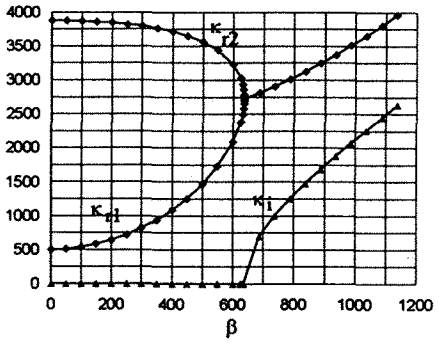

Figure 1. Variation of eigenvalues with respect to flow dynamic pressure : a). Hinged-hinged plate, b). clamped-clamped plae.

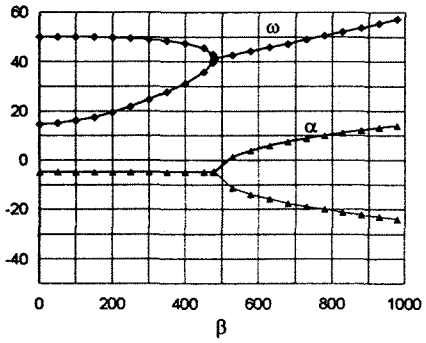

Figure 3. Variation of motion frequency and damping factor with dynamic pressure for case with aerodynamic damping.

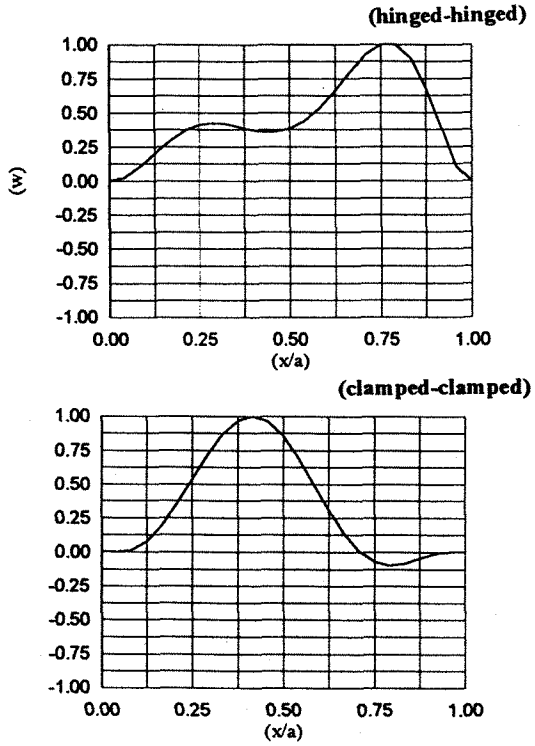

Figure 4. Plate deformation mode at the instability point.

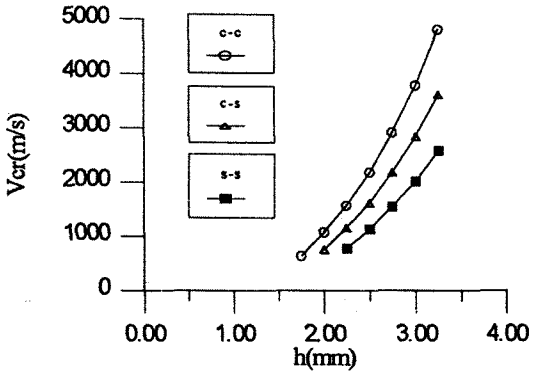

Figure 5. Variation of plate flutter speed with plate thickness.

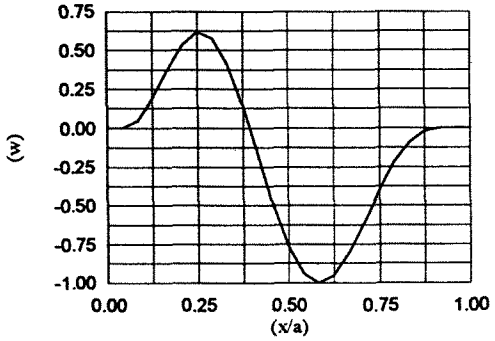

Figure 6. Plate deformation mode at the instability point for plate with four-end conditions.

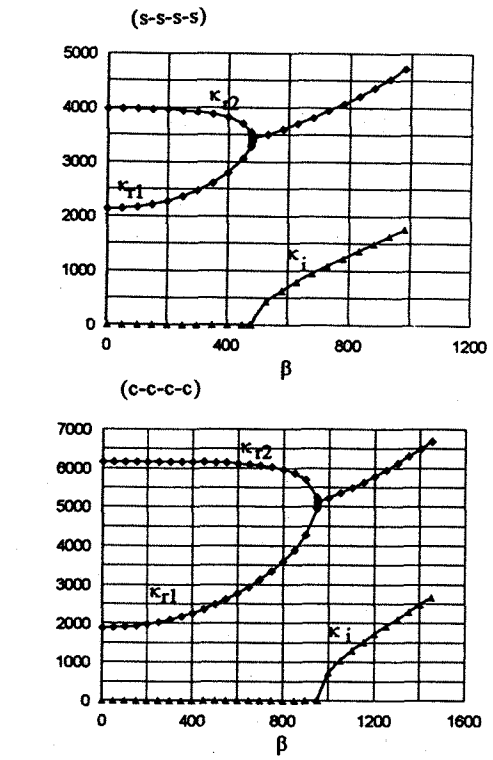

Figure 7. Variation of eigenvalues with respect to flow dynamic pressure for hinged and clamped plate.

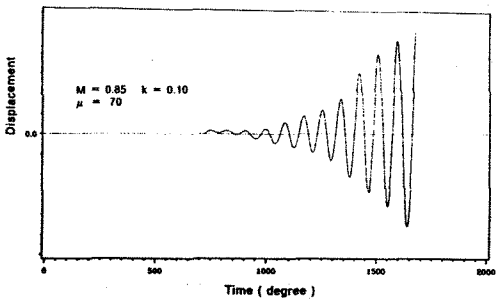

Figure 8. The limit cycle respons of plates.

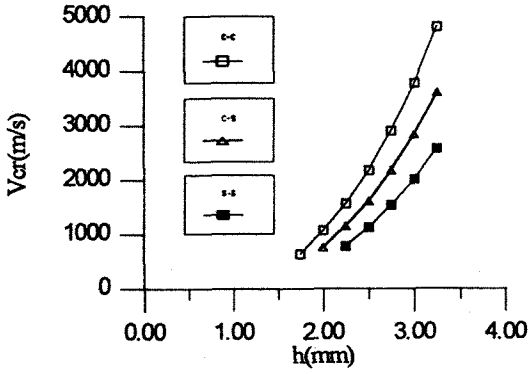

Figure 9. Variation of plate flutter speed with thickness for plate with four-end conditions.